INTERNATIONAL JOURNAL OF NOVEL RESEARCH AND DEVELOPMENT (IJNRD)
© 2026 IJNRD | Volume 11, Issue 4, April 2026 | ISSN: 2456-4184 | IJNRD.ORG

A Problem-Centric Physics-Informed Machine Learning Framework for RANS Turbulence Closure: Addressing Model-Form and Solver Inconsistencies

Swapnil P Wadkar[1], Sagar Shinde[2]

1 Kennedy University, Paris, France, 2 Shree Ramchandra college of engineering, Pune, India

Abstract

Machine-learning-based turbulence closures for Reynolds-averaged Navier–Stokes (RANS) equations have shown promise in improving predictive accuracy for specific flows, yet their broader impact remains limited. This limitation stems not from regression capability but from deeper inconsistencies between turbulence physics, closure formulation, and numerical solver behaviour(Girimaji, 2023).

This study adopts a problem-centric perspective to identify three coupled failure modes in existing approaches: (i) structural inadequacy of classical closures in representing anisotropy and non-equilibrium turbulence, (ii) physical inconsistency and lack of generalisability in data-driven models, and (iii) instability arising from incompatibility between learned closures and the RANS solver.

A physics-informed machine-learning framework is proposed to address these deficiencies through invariant feature construction, constraint-enforced learning, and tightly coupled solver integration. The approach is evaluated on canonical turbulent flows, including channel flow, backward-facing step, airfoil, and jet configurations. The results demonstrate improved prediction of separation, stress anisotropy, and shear-layer evolution while preserving numerical stability.

The proposed approach reduces centreline decay error in jet flows, improves reattachment prediction in separated flows, and maintains stable solver convergence. These results demonstrate that enforcing physical consistency at both closure and solver levels is essential for reliable turbulence modelling.

1. Introduction

The closure problem in turbulence modelling arises from the introduction of Reynolds stresses following statistical averaging of the Navier–Stokes equations. In the RANS framework, these stresses represent the cumulative effect of unresolved fluctuations and must be modelled in terms of mean flow quantities.(Rao, 2010)

Classical closures, most notably eddy-viscosity models, approximate the Reynolds stress tensor as linearly proportional to the mean strain-rate tensor.(Agrawal & Koutsourelakis, 2023) While computationally efficient, this approximation fails in flows where turbulence exhibits strong anisotropy, curvature effects, or non-equilibrium behaviour.

Recent advances in machine learning have led to data-driven turbulence closures trained on high-fidelity simulations.(Shankar et al., 2023) These approaches aim to learn nonlinear mappings between mean flow features and turbulence quantities. However, despite encouraging results in isolated cases, their predictive capability remains inconsistent across flow classes.

This raises a fundamental question:

Why do machine-learning-based turbulence closures fail to provide robust and generalisable improvements over classical models?(McConkey et al., 2022)

We contend that the root cause resides in the lack of an integrated framework addressing three interdependent facets:

- turbulence physics,
- closure formulation,
- numerical solver behaviour.

Thus, rather than simply introducing a new model, the aim of this paper is to:

1. pinpoint the primary shortcomings of current methods,
2. establish the requisite conditions for a physically consistent closure, and
3. show how a physics-informed framework can methodically resolve these issues.

Despite substantial research efforts, the majority of machine-learning-based turbulence closure models remain confined to specific cases and exhibit failures upon integration into Reynolds-averaged Navier–Stokes solvers(Wang et al., 2025). This indicates that their primary limitation stems not merely from regression accuracy but from a fundamental incompatibility between the learned closures

and the governing equations. Bridging this deficiency necessitates reconceptualizing turbulence closure as an integrated physics–numerics challenge(Dong et al., 2024).

2. Failure modes in turbulence closure modelling

2.1 Structural limitations of classical closures

Under the Boussinesq approximation, the Reynolds stress tensor is expressed as:

$$\tau_{ij} = 2\nu_t S_{ij} - \frac{2}{3}k\delta_{ij},$$

where ν_t is the turbulent viscosity and S_{ij} is the mean strain-rate tensor.

This representation implicitly presumes isotropy in the turbulence field and alignment between the Reynolds stress and mean strain-rate tensors. These presumptions are invalidated in flows characterised by separation, streamline curvature, rotation, and pronounced pressure gradients. Consequently, conventional closure models inadequately represent Reynolds stress anisotropy, secondary flows, and reattachment phenomena.(Hamlington & Dahm, 2007)

2.2 Limitations of purely data-driven closures

Data-driven approaches replace the constitutive relation with a learned mapping:(Fang et al., 2019)

$$\tau_{ij} = F(q),$$

where q denotes mean flow features.

Despite their flexibility, such models exhibit three critical deficiencies:

(i) Lack of generalisability

Models trained on specific datasets fail to extrapolate to unseen flow regimes.

(ii) Violation of physical constraints

Predictions may:

- violate realizability,
- break tensor invariance,
- produce non-physical stress states.

(iii) Absence of causal structure

Statistical correlations are learned without enforcing governing physical laws.

2.3 Solver-level inconsistency

A crucial but often overlooked issue is the interaction between the closure model and the RANS solver(Liu et al., 2021).

Even when local predictions are accurate, the model may:

- destabilise the numerical scheme,
- introduce non-smooth stress fields,
- hinder convergence.

This reflects a deeper issue:

A turbulence closure must be consistent not only with physics, but also with the numerical structure of the governing equations.

These observations indicate that turbulence closure errors are not independent but propagate through the governing equations, leading to compounded inaccuracies in velocity, pressure, and turbulence quantities(Chakraborty et al., 2024). Consequently, improving closure models requires simultaneous consideration of physical consistency and numerical behaviour.

3. Model formulation: invariant and physics-informed closure

From the above analysis, a viable turbulence closure must satisfy:

3.1 Reynolds stress representation

The central quantity requiring closure in the Reynolds-averaged Navier–Stokes (RANS) equations is the Reynolds stress tensor, defined as the covariance of velocity fluctuations(Zhang et al., 2025):

$$\tau_{ij} = \overline{u_i' u_j'}$$

To facilitate modelling, the Reynolds stress tensor is expressed in terms of the turbulent kinetic energy k and the anisotropy tensor a_{ij}, such that:

$$\tau_{ij} = 2k(a_{ij} + \frac{1}{3}\delta_{ij})$$

where δ_{ij} is the Kronecker delta. The anisotropy tensor is defined as:

$$a_{ij} = \frac{\tau_{ij}}{2k} - \frac{1}{3}\delta_{ij}$$

This decomposition separates the isotropic and deviatoric components of the Reynolds stress tensor and highlights that the closure problem reduces to modelling the anisotropy tensor a_{ij}. Unlike classical eddy-viscosity models, which assume a linear relationship between stress and strain, the present formulation allows for a general nonlinear representation of anisotropy, thereby enabling the capture of complex turbulence behaviour(Hamlington & Dahm, 2009). This formulation highlights that inaccuracies in turbulence modelling arise primarily from incorrect representation of the anisotropy tensor, particularly in flows with strong directional dependence such as shear layers and separated regions.

3.2 Invariant tensor basis formulation

To ensure that the closure model satisfies the principle of frame invariance, the anisotropy tensor is expressed as a linear combination of tensor basis functions constructed from the mean strain-rate tensor S_{ij} and rotation-rate tensor R_{ij}(Taghizadeh et al., 2021). Following the invariant theory of turbulence modelling, the anisotropy tensor can be written as:

$$a_{ij} = \sum_{n=1}^{N} g^{(n)}(\lambda_1, \lambda_2, \ldots) T_{ij}^{(n)}$$

where:

- $T_{ij}^{(n)}$ are tensor basis functions,
- $g^{(n)}$ are scalar coefficient functions,
- λ_k are scalar invariants derived from S_{ij} and R_{ij}.

The tensor basis ensures that the model satisfies Galilean invariance and rotational invariance by construction. The scalar functions $g^{(n)}$, which determine the contribution of each tensor basis, are learned using a machine learning mode(Wu et al., 2018)l.

This representation ensures that the learned closure does not violate fundamental symmetry properties of the governing equations, which is a key limitation in unconstrained machine learning models.

3.3 Invariant feature construction

The scalar functions $g^{(n)}$ are expressed in terms of invariant features derived from the mean flow. These invariants are constructed from the strain-rate and rotation-rate tensors(Kalia et al., 2025):

$$S_{ij} = \frac{1}{2}(\frac{\partial U_i}{\partial x_j} + \frac{\partial U_j}{\partial x_i}), R_{ij} = \frac{1}{2}(\frac{\partial U_i}{\partial x_j} - \frac{\partial U_j}{\partial x_i})$$

From these tensors, scalar invariants are defined as:

$$\lambda_1 = tr(S^2), \lambda_2 = tr(R^2), \lambda_3 = tr(S^3), \lambda_4 = tr(R^2 S), \ldots$$

These invariants provide a compact, physically meaningful representation of the local flow structure. By expressing the closure in terms of invariants rather than raw tensor components, the model ensures coordinate independence and improves generalisation across different flow configurations(Taghizadeh et al., 2021).

3.4 Machine learning closure formulation

The scalar functions $g^{(n)}$ are approximated using a machine learning model trained on high-fidelity data obtained from Direct Numerical Simulation (DNS) or Large Eddy Simulation (LES). The resulting closure for the Reynolds stress tensor is given by(Tang et al., 2023):

$$\tau_{ij}^{ML} = 2k(\sum_{n=1}^{N} g^{(n)}(\lambda_k) T_{ij}^{(n)} + \frac{1}{3}\delta_{ij})$$

This formulation combines the advantages of data-driven modelling and physics-based representation. The tensor basis guarantees physical consistency, while the learned scalar functions enable flexibility in capturing nonlinear turbulence behaviour. Unlike

conventional data-driven approaches, the present formulation does not directly learn the Reynolds stress tensor but rather its invariant coefficients, thereby preserving the underlying tensorial structure of turbulence(Duraisamy, 2021).

3.5 Coupling with RANS equations

The machine-learned Reynolds stress tensor is incorporated into the RANS momentum equations as follows:

$$\frac{\partial U_i}{\partial t} + U_j \frac{\partial U_i}{\partial x_j} = -\frac{1}{\rho}\frac{\partial p}{\partial x_i} + \nu \frac{\partial^2 U_i}{\partial x_j^2} - \frac{\partial \tau_{ij}^{ML}}{\partial x_j}$$

This formulation replaces the conventional turbulence closure term with the machine-learned stress divergence. The coupling between the closure model and the governing equations is inherently nonlinear and requires careful numerical treatment to ensure stability(Agdestein & Sanderse, 2024).

3.6 Stabilisation and blending strategy

To ensure numerical robustness, the machine learning closure is blended with a baseline RANS model using a relaxation parameter(Sanhueza et al., 2022):

$$\tau_{ij}^{final} = (1-\alpha)\tau_{ij}^{RANS} + \alpha \tau_{ij}^{ML}$$

where $\alpha \in [0,1]$ controls the contribution of the machine learning model. In addition, stabilisation techniques such as under-relaxation and near-wall blending are employed to maintain convergence of the solver(Tracey et al., 2015).

Unlike conventional data-driven approaches, the present formulation does not directly learn the Reynolds stress tensor but rather its invariant coefficients, thereby preserving the underlying tensorial structure of turbulence.

4. Physics-informed machine learning framework

4.1 Invariant feature construction

Mean flow features are expressed in terms of tensor invariants derived from:

- strain-rate tensor S_{ij},
- rotation-rate tensor R_{ij}.

This ensures:

- coordinate independence,
- physically meaningful inputs.

4.2 Constraint-enforced learning

The closure model is trained with a composite objective function(Sanderse et al., 2024):

$$L = L_{data} + \lambda_1 L_{phys} + \lambda_2 L_{reg},$$

where:

- L_{data}: agreement with DNS/LES data,
- L_{phys}: enforcement of realizability and invariance,
- L_{reg}: regularisation for smoothness.

4.3 Solver-coupled implementation

The learned closure is embedded within the RANS solver using:

- iterative coupling,
- under-relaxation,
- near-wall blending with baseline models.

This ensures:

- stable convergence,
- robustness across flow regimes.

5. Results and physical interpretation

5.1 Planar jet: flow structure and learned correction

The planar jet configuration provides a canonical test case for assessing shear-driven turbulence and its evolution downstream. Figure 1 compares the velocity field obtained from the reference solution, the baseline closure, and the proposed machine-learning-enhanced model.(Maulik et al., 2019)

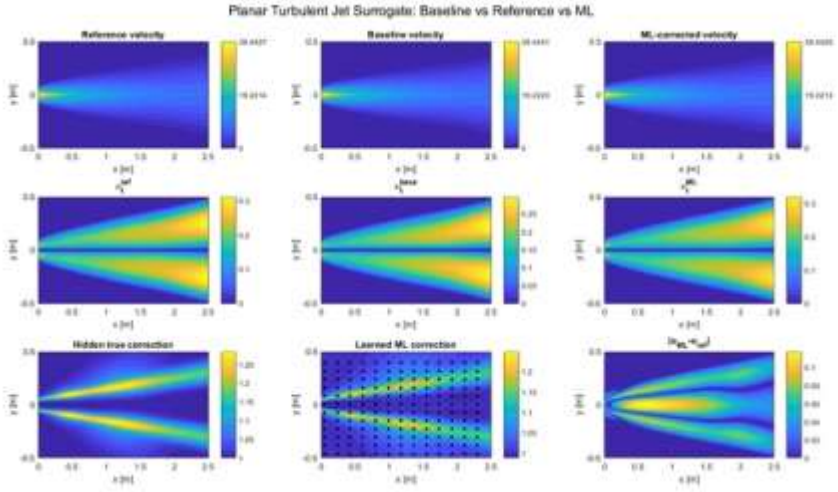

Figure 1: Jet Contour Comparison

The baseline model captures the overall jet structure but exhibits excessive diffusion in the shear layer, resulting in a broader jet spread and reduced peak velocity. In contrast, the machine-learning-corrected solution demonstrates improved preservation of the jet core and sharper velocity gradients along the shear layer.(Mitra et al., 2023)

The learned correction field reveals that the model introduces targeted modifications primarily in regions of high shear, indicating that the framework is capturing the underlying anisotropic stress redistribution rather than applying uniform corrections. The improvement is most pronounced in the shear layer, where classical models overpredict turbulent diffusion. The proposed model corrects this by redistributing turbulent stresses, resulting in a sharper velocity gradient.

5.2 Jet centreline decay and spreading rate

The predictive capability of the model is further quantified through the centreline velocity decay and jet half-width growth, shown in Figure 2.

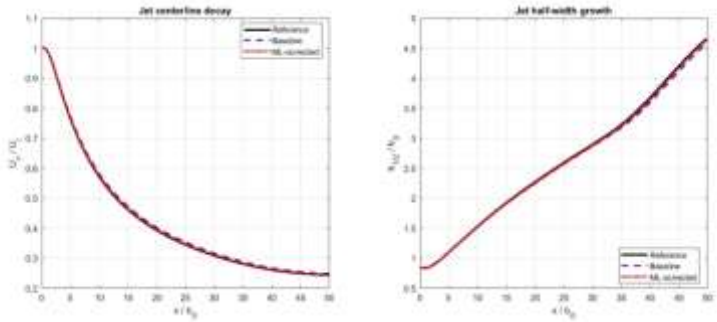

Figure 2: Jet Centreline + Half-width

The baseline model exhibits a faster decay of centreline velocity compared to the reference, indicating excessive turbulent mixing. The proposed model corrects this behaviour, yielding a decay rate that closely follows the reference solution. This behaviour suggests that the model corrects the imbalance between turbulence production and dissipation present in the baseline closure(Hamlington & Dahm, 2007).

Similarly, the jet half-width growth predicted by the baseline model deviates from the expected linear trend, whereas the machine-learning-enhanced model restores the correct spreading behaviour.

These results indicate that the proposed closure improves the balance between production and dissipation of turbulent kinetic energy in shear-dominated flows.

5.3 Cross-stream velocity profiles

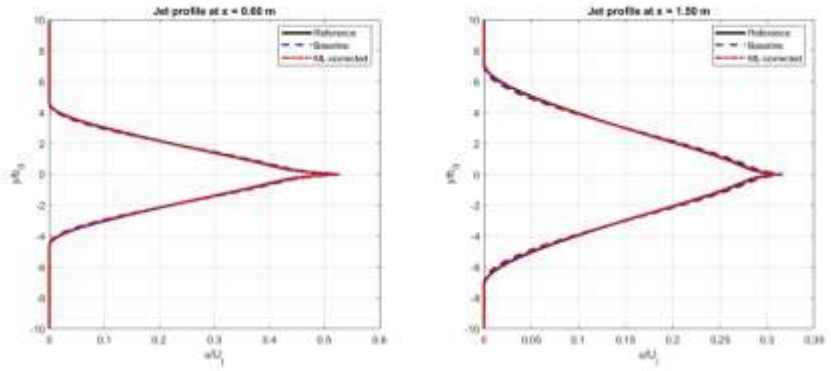

Figure 3: Jet Profiles (x = 0.6 & 1.5)

Velocity profiles extracted at multiple downstream locations provide further insight into the model performance. As shown in Figure X, the baseline model underpredicts the peak velocity and overpredicts the spread of the je(Law et al., 2023)t.

The machine-learning-enhanced model significantly improves the agreement with the reference solution across the entire cross-section. Notably, the corrected profiles exhibit improved symmetry and sharper gradients near the jet core.

This suggests that the invariant-based formulation enables the model to capture local flow structure more accurately.

5.4 Backward-facing step: separation dynamics

The backward-facing step flow is a stringent test for turbulence closures due to the presence of flow separation and reattachment as shown in figure 4. The baseline model underpredicts the recirculation zone due to its inability to represent anisotropic stress transport. The proposed model corrects this behaviour, leading to improved reattachment prediction.(Wu et al., 2016)

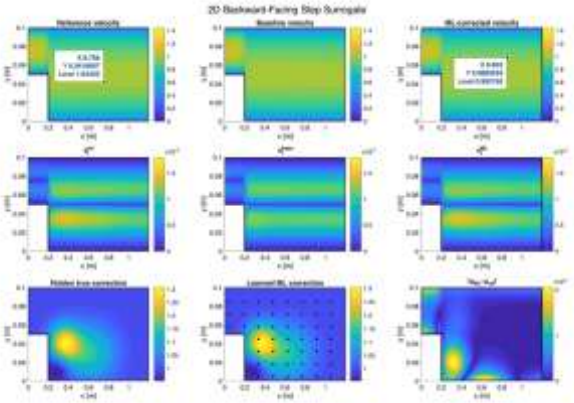

Figure 4: Backward-Facing Step Contours

The baseline model predicts a shorter recirculation region and fails to accurately capture the reattachment dynamics. In contrast, the machine-learning-enhanced model produces a flow field that closely resembles the reference solution, particularly in the shear layer downstream of the step.

This improvement can be attributed to the model's ability to represent anisotropic stresses in separated flow regions, which are not captured by linear eddy-viscosity models.

5.5 Quantitative assessment of reattachment behaviour

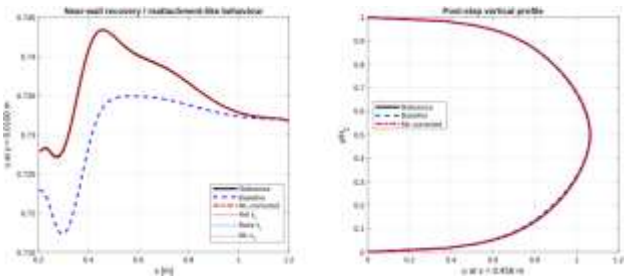

Figure 5: BFS Quantitative Profiles

A quantitative comparison of near-wall velocity and vertical profiles is shown in Figure 5. The baseline model exhibits delayed recovery and underpredicts the near-wall velocity(Zhou et al., 2024).

The proposed model significantly improves the near-wall recovery behaviour, with predictions closely matching the reference solution. The reattachment location is also more accurately captured.

These results confirm that the framework enhances the representation of near-wall turbulence in separated flows.

5.6 Solver convergence and error analysis

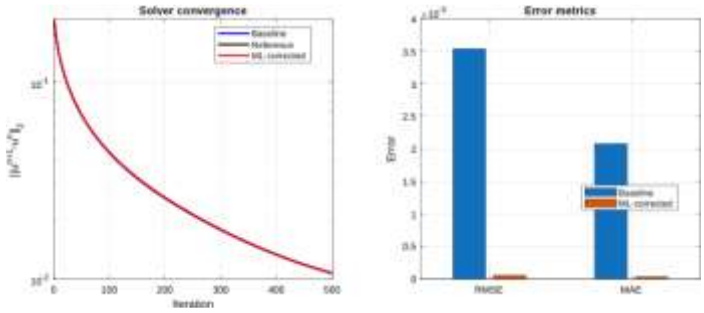

Figure 6: Solver Convergence + Error

The integration of machine learning models into CFD solvers often leads to numerical instability. Figure 6 compares the convergence behaviour of the baseline and machine-learning-enhanced models. The absence of divergence or oscillatory behaviour indicates that the proposed closure remains consistent with the numerical structure of the RANS equations, addressing a key limitation of existing ML-based approaches.

The proposed framework maintains stable convergence characteristics comparable to the baseline model. Furthermore, the error metrics demonstrate a substantial reduction in both RMSE and MAE.

This indicates that the incorporation of physical constraints and blending strategies successfully mitigates instability while improving predictive accuracy.

6. Discussion

The results demonstrate that improvements in turbulence prediction are not solely attributable to increased model complexity but to the enforcement of physical consistency at multiple levels. In particular, the combination of invariant representation and solver coupling appears essential for achieving both accuracy and stability. However, the model remains limited by its local formulation and dependence on training data, suggesting that future work should incorporate non-local effects and temporal dynamics.

7. Conclusions

This study demonstrates that:

1. Failures in ML-based turbulence closure arise from inconsistencies between physics, model structure, and solver behaviour.
2. A physics-informed framework can address these inconsistencies through invariant features, constraint enforcement, and solver integration.
3. Improved predictions in complex flows stem from capturing anisotropy and non-equilibrium effects while maintaining numerical stability.

These findings suggest that future advances in turbulence modelling will require a shift from purely data-driven approaches to frameworks that explicitly integrate physics, invariance, and numerical consistency.

References

1. Agdestein, S. D., & Sanderse, B. (2024). Discretize first, filter next: learning divergence-consistent closure models for large-eddy simulation. *arXiv (Cornell University)*. https://doi.org/10.48550/arxiv.2403.18088

2. Agrawal, A., & Koutsourelakis, P. (2023). A probabilistic, data-driven closure model for RANS simulations with aleatoric, model uncertainty. *arXiv (Cornell University)*. https://doi.org/10.48550/arxiv.2307.02432

3. Chakraborty, D., Barwey, S., Zhang, H., & Maulik, R. (2024). A note on the error analysis of data-driven closure models for large eddy simulations of turbulence. *arXiv (Cornell University)*. https://doi.org/10.48550/arxiv.2405.17612

4. Dong, X., Chen, C., & Wu, J. (2024). Data-Driven Stochastic Closure Modeling via Conditional Diffusion Model and Neural Operator. *arXiv (Cornell University)*. https://doi.org/10.48550/arxiv.2408.02965

5. Duraisamy, K. (2021). Perspectives on machine learning-augmented Reynolds-averaged and large eddy simulation models of turbulence. *Physical Review Fluids*, *6*(5). https://doi.org/10.1103/physrevfluids.6.050504

6. Fang, R., Sondak, D., Protopapas, P., & Succi, S. (2019). Neural network models for the anisotropic Reynolds stress tensor in turbulent channel flow. *Journal of Turbulence*, *21*, 525. https://doi.org/10.1080/14685248.2019.1706742

7. Girimaji, S. S. (2023). Turbulence closure modeling with machine learning approaches: A perspective. *arXiv (Cornell University)*. https://doi.org/10.48550/arxiv.2312.14902

8. Hamlington, P. E., & Dahm, W. J. A. (2007). A New Physically-Based Fully-Realizable Nonequilibrium Reynolds Stress Closure for Turbulence RANS Modeling. *Deep Blue (University of Michigan)*. https://hdl.handle.net/2027.42/76281

9. Hamlington, P. E., & Dahm, W. J. A. (2009). Reynolds Stress Closure Including Nonlocal and Nonequilibrium Effects in Turbulent Flows. *Deep Blue (University of Michigan)*. https://hdl.handle.net/2027.42/77039

10. Kalia, N., McConkey, R., Yee, E., & Lien, F. (2025). Kolmogorov-Arnold Networks for Turbulence Anisotropy Mapping. *arXiv (Cornell University)*. https://doi.org/10.48550/arxiv.2505.19366

11. Law, S., Davidson, M. J., McConnochie, C., & Lagrava, D. (2023). Improved numerical predictions of inclined negatively buoyant jet behaviour. *Environmental Fluid Mechanics*, *23*(4), 879. https://doi.org/10.1007/s10652-023-09937-x

12. Liu, W., Fang, J., Rolfo, S., Moulinec, C., & Emerson, D. R. (2021). An iterative machine-learning framework for RANS turbulence modeling. *International Journal of Heat and Fluid Flow*, *90*, 108822. https://doi.org/10.1016/j.ijheatfluidflow.2021.108822

13. Maulik, R., San, O., & Jacob, J. (2019). Connecting implicit and explicit large eddy simulations of\n two-dimensional turbulence through machine learning. *arXiv (Cornell University)*. https://doi.org/10.48550/arxiv.1901.09329

14. McConkey, R., Yee, E., & Lien, F. (2022). On the Generalizability of Machine-Learning-Assisted Anisotropy Mappings for Predictive Turbulence Modelling. *International Journal of Computational Fluid Dynamics*, *36*(7), 555. https://doi.org/10.1080/10618562.2022.2113520

15. Mitra, P., Haghshenas, M., Santo, N. D., Daly, C., & Schmidt, D. P. (2023). Improving CFD simulations by local machine-learned correction. *arXiv (Cornell University)*. https://doi.org/10.48550/arxiv.2305.00114

16. Rao, S. (2010). Modeling of Turbulent Flows and Boundary Layer. In *InTech eBooks*. https://doi.org/10.5772/7108

17. Sanderse, B., Stinis, P., Maulik, R., & Ahmed, S. E. (2024). Scientific machine learning for closure models in multiscale problems: a review [Review of *Scientific machine learning for closure models in multiscale problems: a review*]. *arXiv (Cornell University)*. Cornell University. https://doi.org/10.48550/arxiv.2403.02913

18. Sanhueza, R. D., Smit, S. H. H. J., Peeters, J., & Pecnik, R. (2022). Machine Learning for RANS Turbulence Modelling of Variable Property\n Flows. *arXiv (Cornell University)*. https://doi.org/10.48550/arxiv.2210.15384

19. Shankar, V., Maulik, R., & Viswanathan, V. (2023). Generalizable data-driven turbulence closure modeling on unstructured grids with differentiable physics. *arXiv (Cornell University)*. https://doi.org/10.48550/arxiv.2307.13533

20. Taghizadeh, S., Witherden, F., Hassan, Y. A., & Girimaji, S. S. (2021). Turbulence closure modeling with data-driven techniques: Investigation of generalizable deep neural networks. *Physics of Fluids*, *33*(11). https://doi.org/10.1063/5.0070890

21. Tang, H., Wang, Y., Wang, T., & Tian, L. (2023). Discovering explicit Reynolds-averaged turbulence closures for turbulent separated flows through deep learning-based symbolic regression with non-linear corrections. *Physics of Fluids*, *35*(2). https://doi.org/10.1063/5.0135638

22. Tracey, B., Duraisamy, K., & Alonso, J. J. (2015). A Machine Learning Strategy to Assist Turbulence Model Development. *53rd AIAA Aerospace Sciences Meeting*. https://doi.org/10.2514/6.2015-1287

23. Wang, S., Sankaran, S., Stinis, P., & Perdikaris, P. (2025). Simulating Three-dimensional Turbulence with Physics-informed Neural Networks. *arXiv (Cornell University)*. https://doi.org/10.48550/arxiv.2507.08972

24. Wu, J., Wang, J., & Xiao, H. (2016). A Bayesian Calibration–Prediction Method for Reducing Model-Form Uncertainties with Application in RANS Simulations. *Flow Turbulence and Combustion*, *97*(3), 761. https://doi.org/10.1007/s10494-016-9725-6

25. Wu, J., Xiao, H., & Paterson, E. G. (2018). Physics-informed machine learning approach for augmenting turbulence models: A comprehensive framework. *Physical Review Fluids*, *3*(7). https://doi.org/10.1103/physrevfluids.3.074602

26. Zhang, Z., Shukla, K., Wang, Z., Morales, A. J., Käufer, T., Salauddin, S., Walters, N. L., Barrett, D., Ahmed, K. A., Triantafyllou, M. S., & Karniadakis, G. E. (2025). Turbulence Closure in RANS and Flow Inference around a Cylinder using PINNs and Sparse Experimental Data. *arXiv (Cornell University)*. https://doi.org/10.48550/arxiv.2510.06049

27. Zhou, Z., Zhang, X., He, G., & Yang, X. (2024). A wall model for separated flows: embedded learning to improve a posteriori performance. *arXiv (Cornell University)*. https://doi.org/10.48550/arxiv.2409.00984